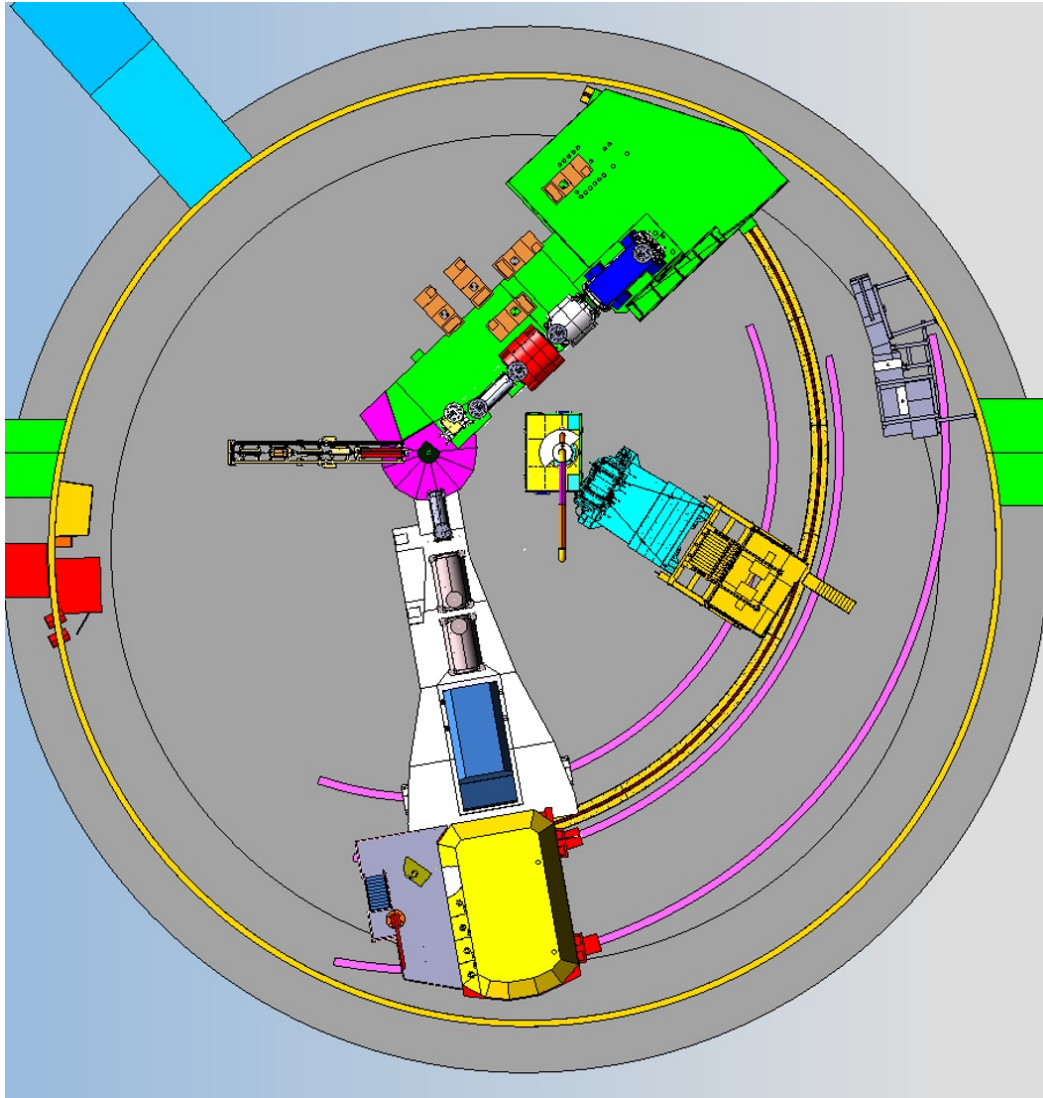


Next years SBS experiments

Bogdan Wojtsekhowski, for the SBS collaboration

The SBS layout in Hall C

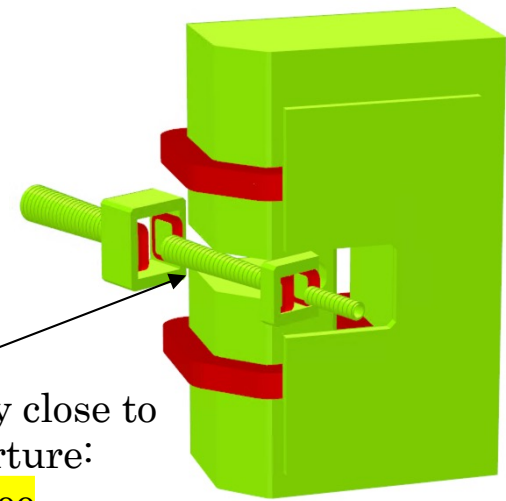
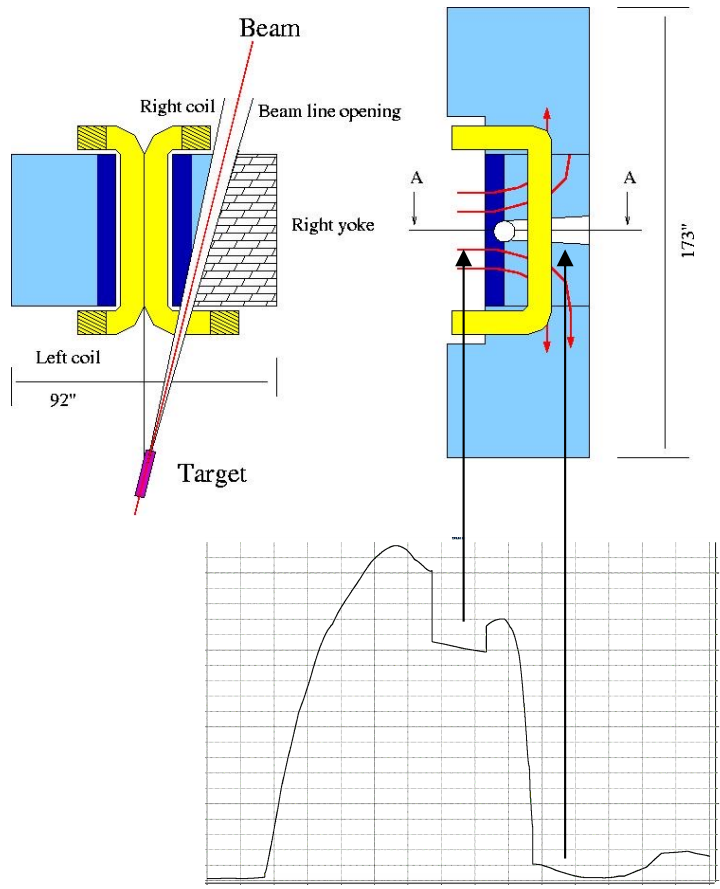


The target is moved downstream by 3 m

SBS magnet need to be moved up according to level of the beam line
In Hall C

Super Bigbite Spectrometer

SBS concept in Feb. 2007, BW for GEp

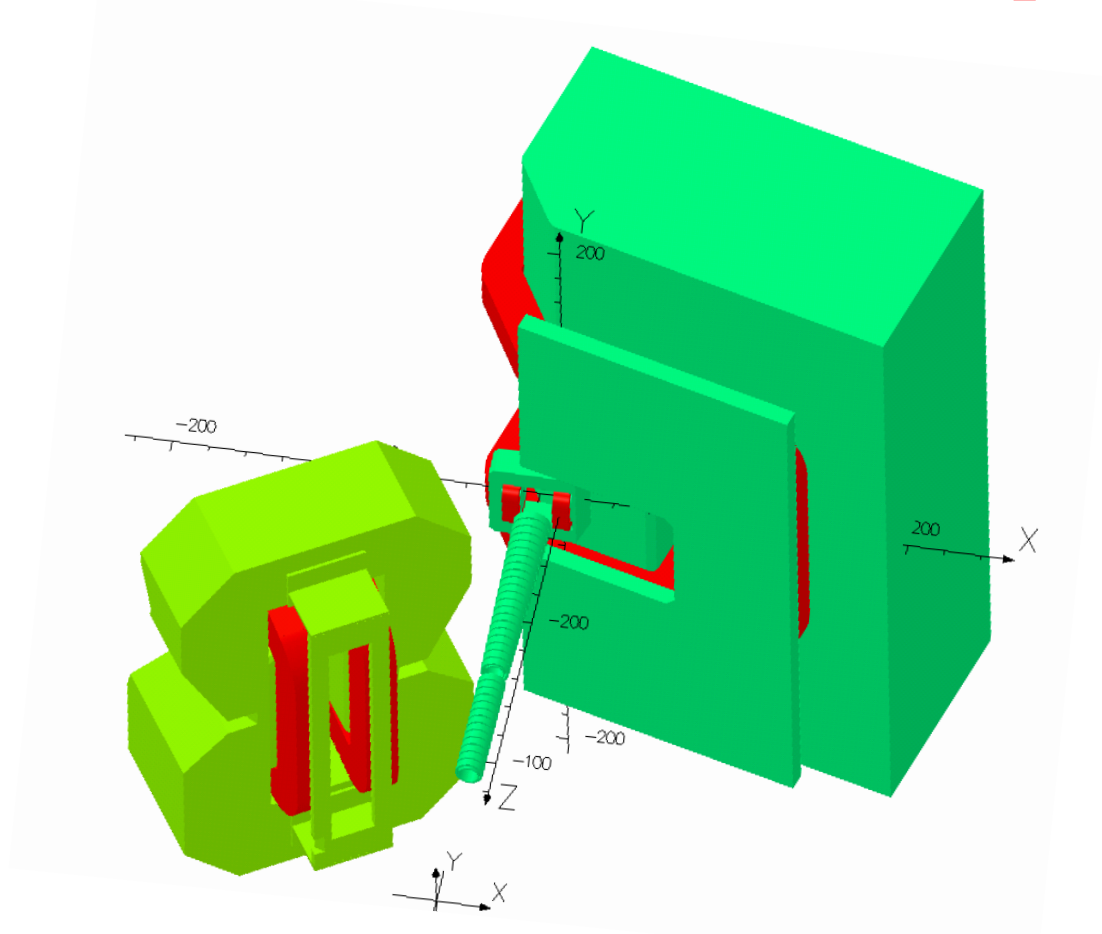


Beam line is very close to the detector aperture: down to 2.2 degree

$\theta_{central}$, degree	Ω , msr	D, meter	Hor. range, degree	Vert. range, degree
3.5	5	9.5	± 1.3	± 3.3
5.0	12	5.8	± 1.9	± 4.9
7.5	30	3.2	± 3	± 8
15	72	1.6	± 4.8	± 12.2
30	76	1.5	± 4.9	± 12.5

At forward angle 15 deg SBS covers 22% of the full 2π azimuthal angle

Two-arm SBS/BB setup



$$\begin{aligned}\sigma_p/p &= 0.08 + 0.004 \times p[\text{GeV}] \\ \sigma_\theta &= 1 - 2, \text{ mrad} \\ \Omega &= 70 - 90 \text{ msr, for } \theta \geq 30^\circ\end{aligned}$$

$$\begin{aligned}\sigma_p/p &= 0.0029 + 0.0003 \times p[\text{GeV}] \\ \sigma_\theta &= 0.14 + 1.3/p[\text{GeV}], \text{ mrad} \\ \Omega &= 72 \text{ msr, for } \theta \geq 15^\circ \\ \Omega &= 30 \text{ msr, for } \theta = 7.5^\circ\end{aligned}$$

Two-arm SBS/BB setup for $e, e'x$

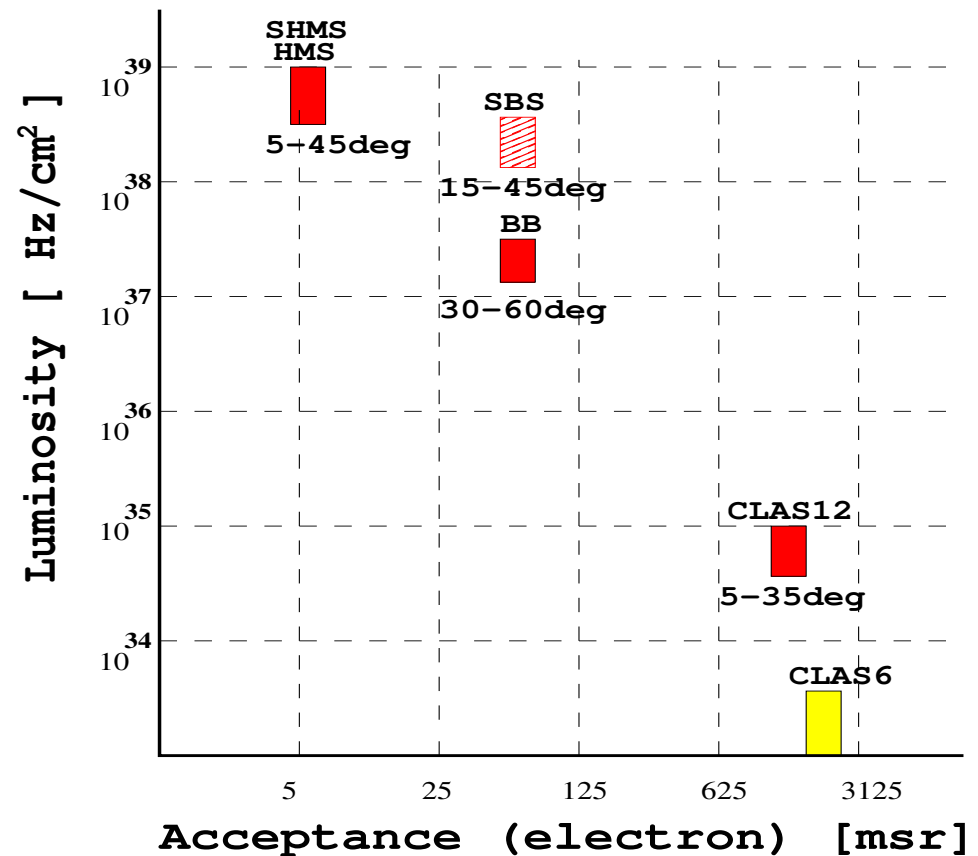
A typical two-body final state process ($e, e'x$): Elastic FF, DVCS, SIDIS, Compton, ...

Relative range of $\Delta Q^2/Q^2 \sim 0.1$

Range of $z \sim P_X / |q| \sim 0.75-1$

Range of $P_{\text{perp}} / P_X \sim 0.1$

Effectively FOM is defined by acceptance of the one arm



One- and Two-Arm experiments (O&TA)

Many productive experiments in the field belong to
the **category One- and Two-Arm**:

Among them are DIS, SIDIS, FFs (GEP), WACS, DVCS,

The main advantage of these “simple” (e,e’) and (e,e’h/g) is
the **simplicity** of such processes for physics interpretation

The productivity of an experiment or Figure-of-Merit:

$$FOM = \mathcal{L} \times \Omega_1 (\times \Omega_2)$$

One- and Two-Arm experiments (O&TA)

$$FOM = \mathcal{L} \times \Omega_{electron} = 10^{38} \cdot 0.07 = 7 \times 10^{36}$$

electron/s × nucleon/cm² × sr

Now we can formulate detector configuration for productive one- and two-arm experiments

- Magnetic analysis with “vertical bend”
- Moderate solid angle >> universal spectrometer
- Independent arms
- Small angle capability down to 3.5 degree
- Space behind magnet for segmented PID, polarimeter

One- and Two-Arm experiments (O&TA)

$$FOM = \mathcal{L} \times \Omega_{electron} = 10^{38} \cdot 0.07 = 7 \times 10^{36}$$

electron/s × nucleon/cm² × sr

Now we can formulate detector configuration
for productive one- and two-arm experiments

- Magnetic analysis with “vertical bend”
 - Moderate solid angle
 - Independent arms
 - Small angle capability
 - Space for segmented PID, polarimeter
- => “protected” detector
=> on level of 20% of 2π
=> full range of angles
=> high x, t, low x
=> RICH counter, HCAL*

Where is SBS/BB system useful?

In the process with one or two particles final state

- High Q^2 , e.g. elastic nucleon form factors, GMn-18, DVCS
- Large acceptance, e.g. polarized target He-3, NH₃/ND₃: g1/g2
- Two-arm high-z experiments, e.g. SIDIS, H(e,e'φ), D(γ,pn)
- Large acceptance high luminosity, e.g. AVFF, pEMC

The SBS physics program

- GEP : will reach $12 (\text{GeV}/c)^2$
- GMN: reach $13.5 (\text{GeV}/c)^2$ and nTPE at $4 (\text{GeV}/c)^2$
- GEN: reach $10 (\text{GeV}/c)^2$
- KLL (pion photo-production at high s/t/u)
- GEn-RP at $4 (\text{GeV}/c)^2$
- GEp+ $3.7 (\text{GeV}/c)^2$, for TPE with positron beam

-
-
- SSA in nSIDIS: 30,000 gain vs HERMES - approved
 - polarized WACS -- A_{LL} - approved
 - Strange FF at $2.5 (\text{GeV}/c)^2$ - approved

- Tagged DIS – luminosity 100 x BONUS – on the way to approval
- Axial Vector FF -- presented to Hall C 1/13
- GMn-18 – presented to Hall C 1/14
- $H(e, e'\phi)$ -- DVVM – presented to Hall C 1/14
- $D(e, e'n_s)$ – proton EMC – presented to Hall C 1/14

- GEn-RP at 7-8 $(\text{GeV}/c)^2$ – needs to be developed
- Deuteron physics: SBS + NH_3/ND_3

The SBS physics in Hall C

- SSA in nSIDIS: 30,000 gain vs HERMES - approved
- polarized WACS -- - approved
- Strange FF at 2.5 (GeV/c)² - approved

- Tagged DIS – luminosity 100 x BONUS – on the way to full approval
- Axial Vector FF – proposal for PAC53 writing
- GMn-18 – LOI for PAC53
- H(e,e'φ) -- DVVM – presented to Hall C 1/14
- D(e,e'n_s) – proton/neutron EMC – LOI for PAC53

- GEn-RP at 7-8 (GeV/c)² – needs to be developed
- Deuteron physics: SBS + NH₃/ND₃

The goal is understanding of the nucleon

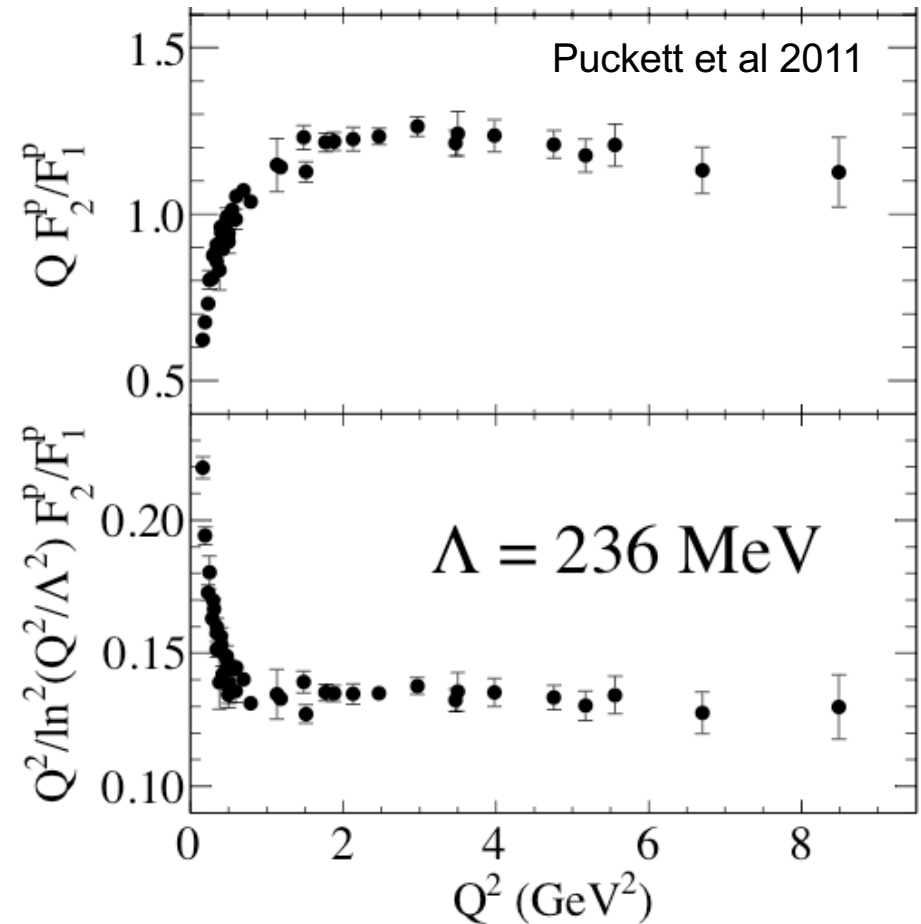
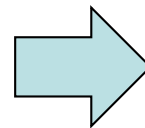
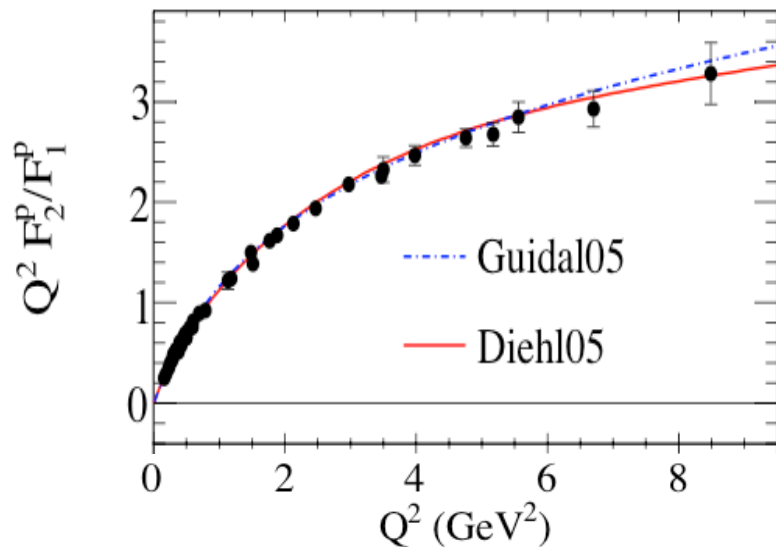
From the Sachs FFs to the ratio F_2/F_1 and the Belitsky, Ji, Yuan “log” scaling

Orbital moment !

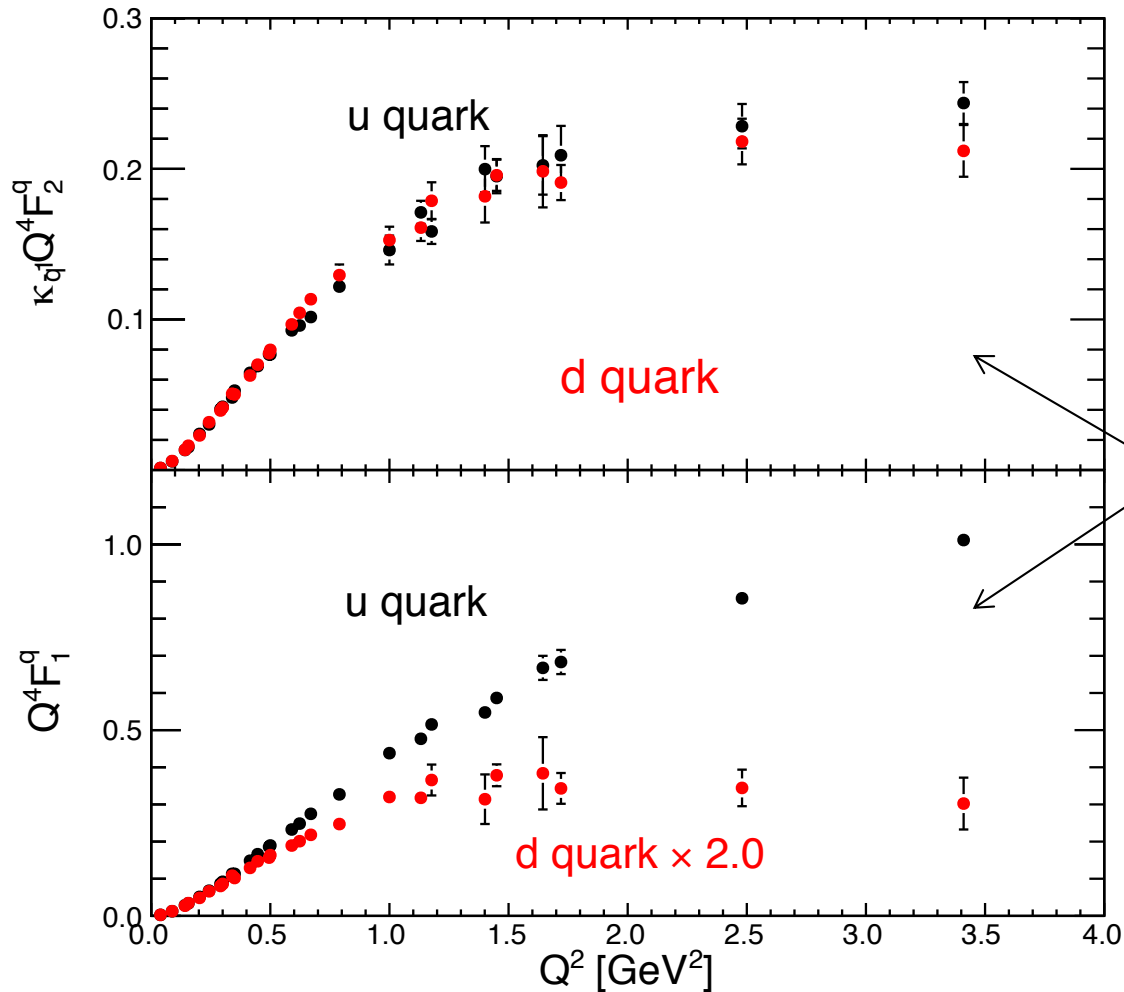
$$F_1 = \frac{G_E + \tau G_M}{1 + \tau} \quad F_2 = -\frac{G_E - G_M}{1 + \tau}$$

$$\tau = Q^2/4M^2$$

$$Q^2 F_2/F_1 \propto \frac{1 - G_E/G_M}{1 + [G_E/G_M]/\tau}$$



Flavor contributions to the nucleon FFs



CJRW (u/d from elastic form factors)
 Phys. Rev. Lett. 106 (2011)

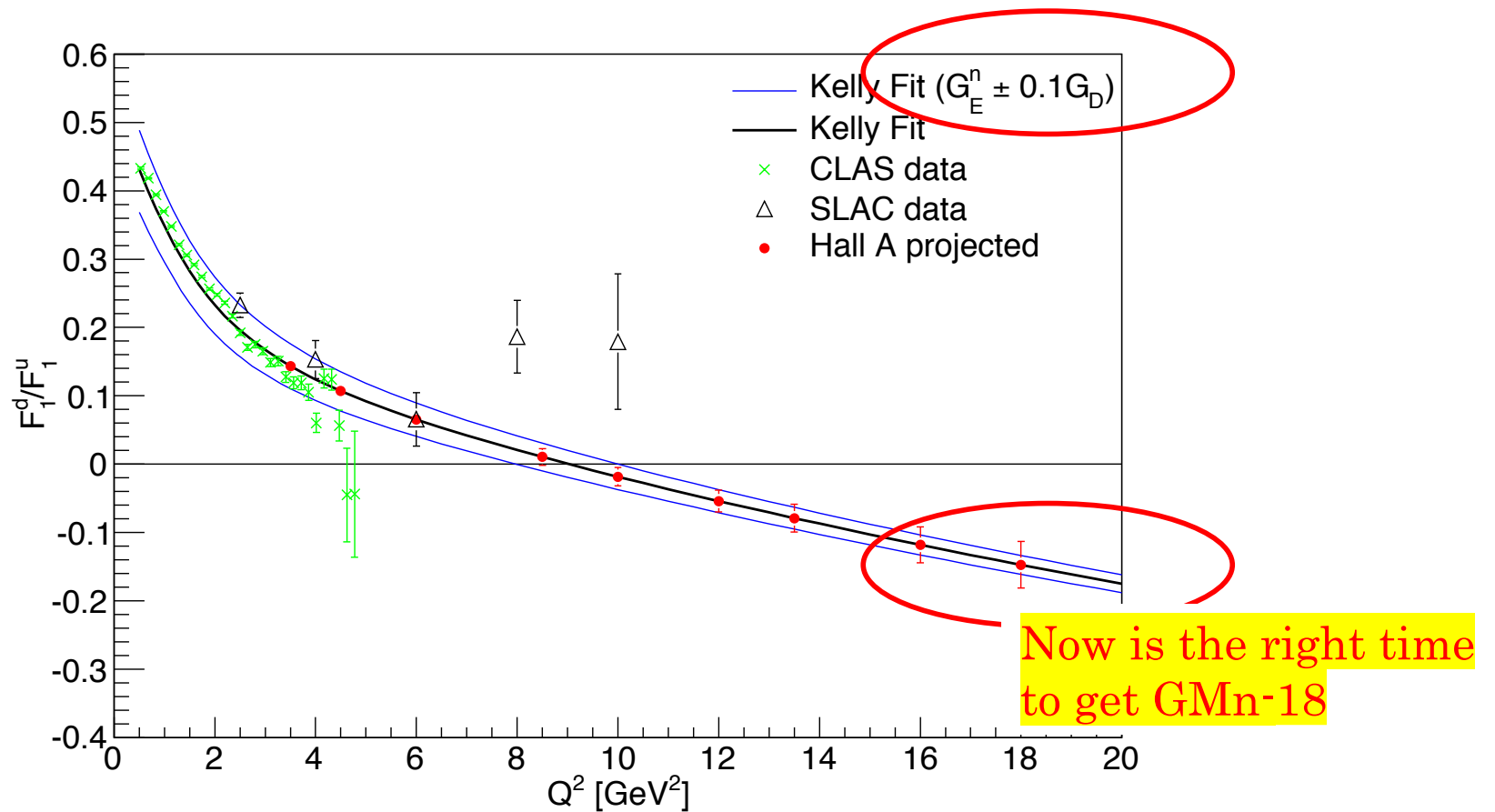
M. Diehl and P. Kroll (GPDs)
 Eur. Phys. J. C73 (2013) 2397

Using the D&K table of F^u , F^d

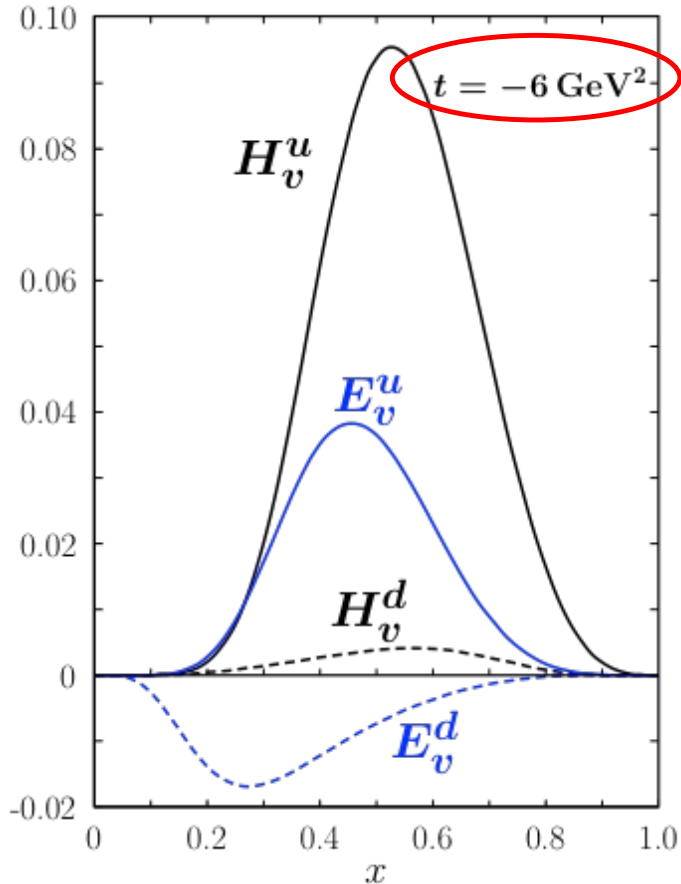
The down quark contribution to the F_1 proton form factor is strongly suppressed at high Q^2

F_1 decomposition at very large Q^2

$$F_1 = \frac{G_E + \tau G_M}{1 + \tau} \quad F_2 = -\frac{G_E - G_M}{1 + \tau}$$



Diehl-Kroll GPDs analysis (2013)



$$F_1(t) = \sum_q e_q \int dx H_q(x, t)$$

$$q(x, \mathbf{b}) = \int \frac{d^2 q}{(2\pi)^2} e^{i \mathbf{q} \cdot \mathbf{b}} H_q(x, t = -q^2)$$

$$\rho(\mathbf{b}) \equiv \sum_q e_q \int dx q(x, \mathbf{b}) = \int d^2 q F_1(q^2) e^{i \mathbf{q} \cdot \mathbf{b}}$$

$$\rho(\mathbf{b}) = \int_0^\infty \frac{Q \cdot dQ}{2\pi} J_0(Qb) \frac{G_E(Q^2) + \tau G_M(Q^2)}{1 + \tau}$$

$$\text{center of momentum } \mathbf{R}_\perp = \sum_i \mathbf{x}_i \cdot \mathbf{r}_{\perp, i}$$

\mathbf{b} is defined relative to \mathbf{R}_\perp

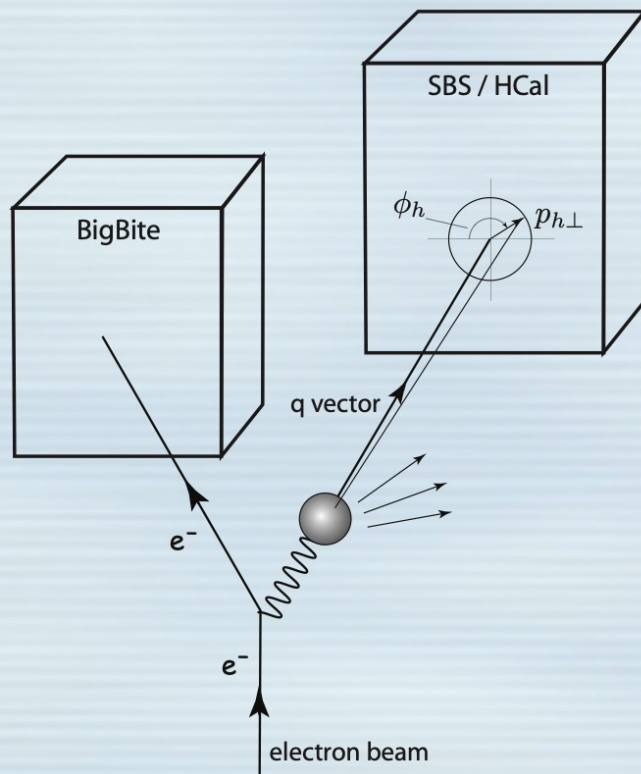
At $-t = 6 \text{ GeV}^2$ H^d is 12 times smaller than H^u

Positive $H^d \Rightarrow$ negative F_1^d

SIDIS, E12-09-018

G. Cates, E. Cisbani, G. Franklin, A. Puckett, B. Wojtsekhowski

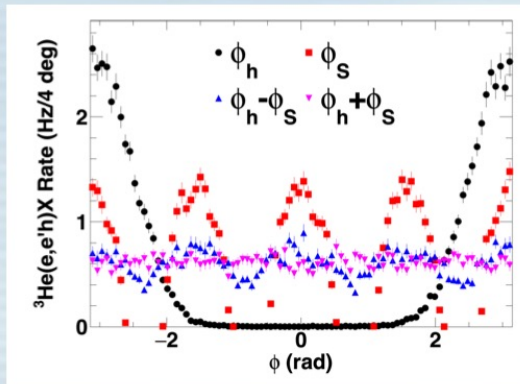
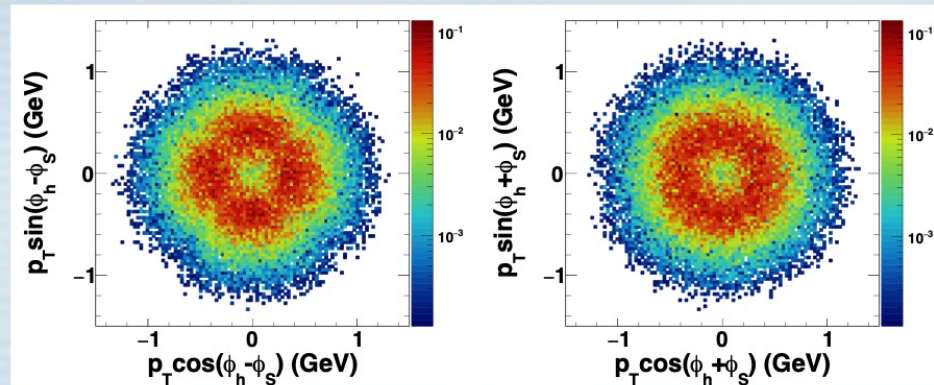
The concept behind the SBS SIDIS experiment



- The open-geometry dipole spectrometers allow wide kinematic coverage with a single setting.
- GEM-based tracking can handle huge singles rates.
- Center the hadron arm on q
- Exploit kinematic focusing along q
- Polarized ^3He target has flexibility to orient polarization relatively freely in the plane perpendicular to q .

By judicious positioning of the hadron arm, even moderate solid angle results in excellent statistics.

SBS SIDIS Azimuthal Coverage

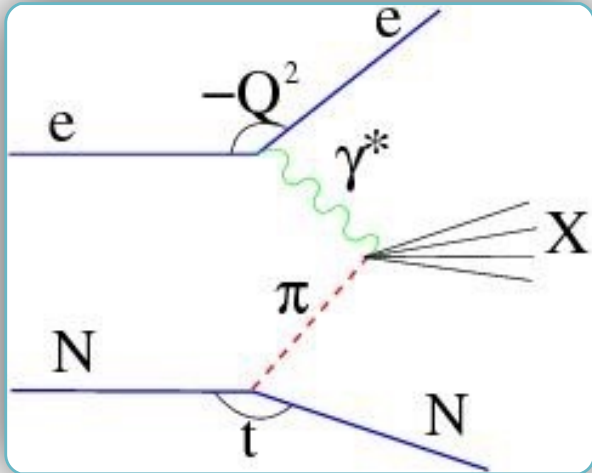


- Our original proposal envisioned eight spin orientations.
- We find virtually unchanged azimuthal coverage (and overall FoM) with four.
- Limiting to four spin orientations greatly simplifies the polarized target, enabling the use of major portions of the G_{E^N} target.

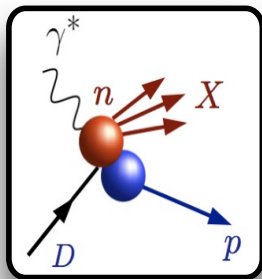
Tagged DIS, C12-14-010

J. Arrington, C. Ayerbe Gayoso, D. Dutta, E. Fuchey, T. Horn, C. Keppel, P. King, N. Liyanage, S. Li, R. Montgomery, A. Tadepalli, B. Wojtsekhowski

The Sullivan process

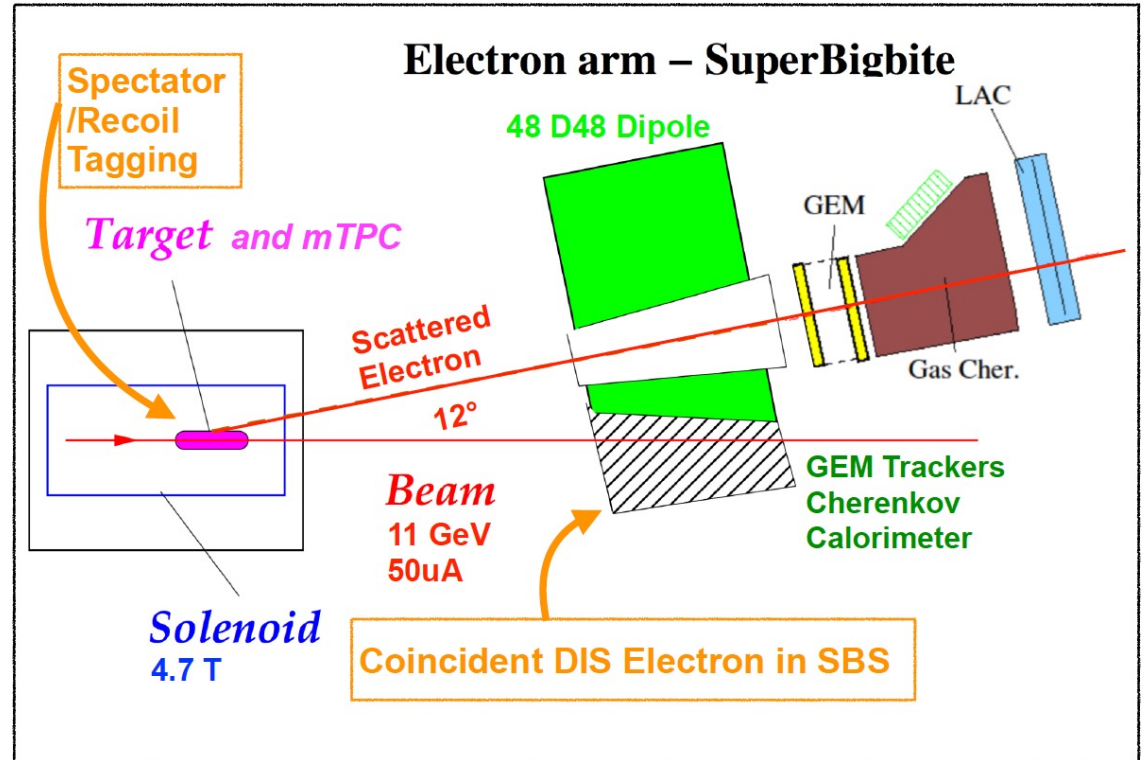


almost free neutron



Deuteron

Spectator proton



TDIS is a pioneering experiment that will provide the first direct measure of the mesonic content of nucleons.

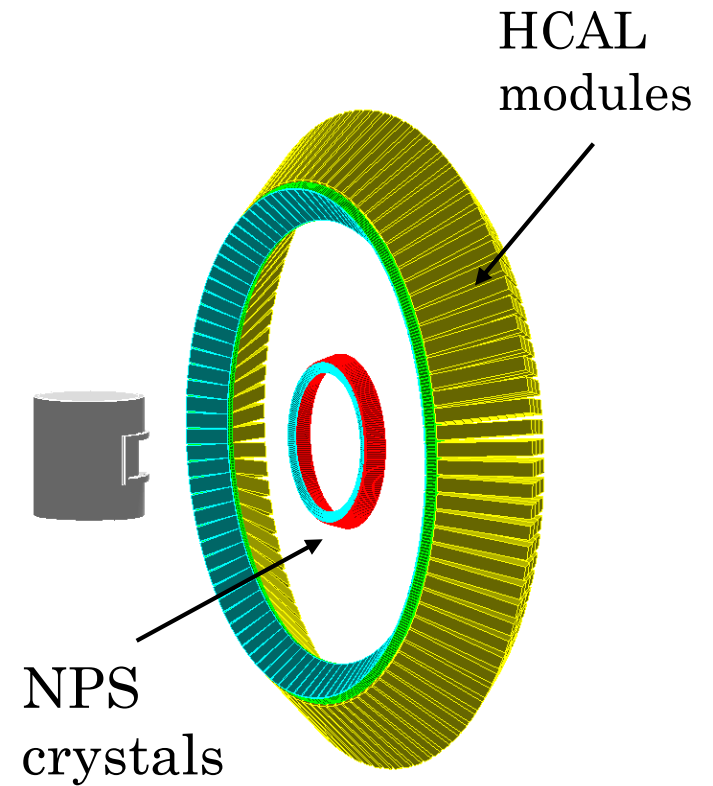
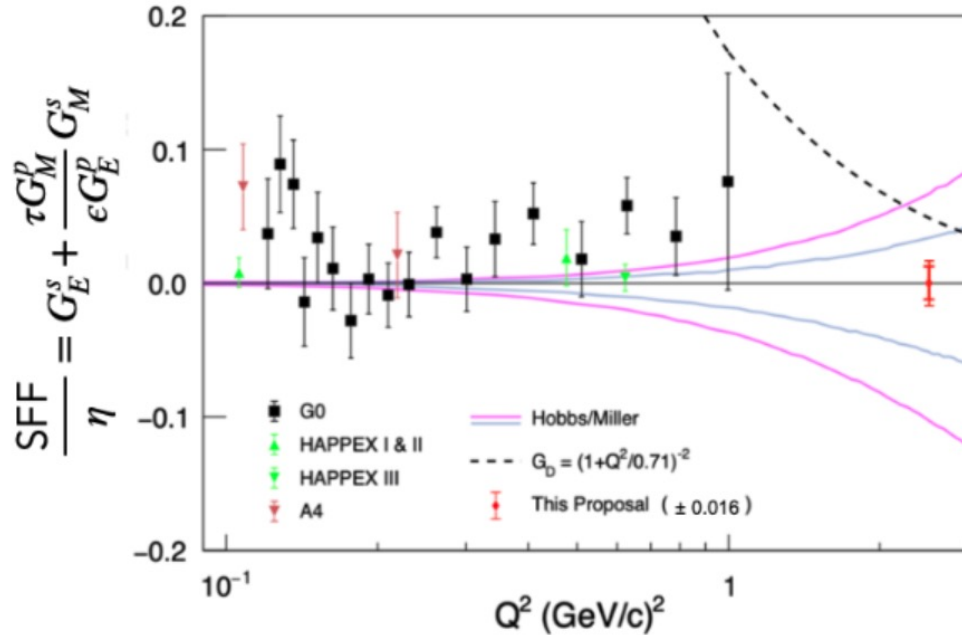
The technique used to extract meson structure function is a necessary first step for future experiments at the EIC & 22 GeV JLab.

Nonzero Strange FF, E12-23-004

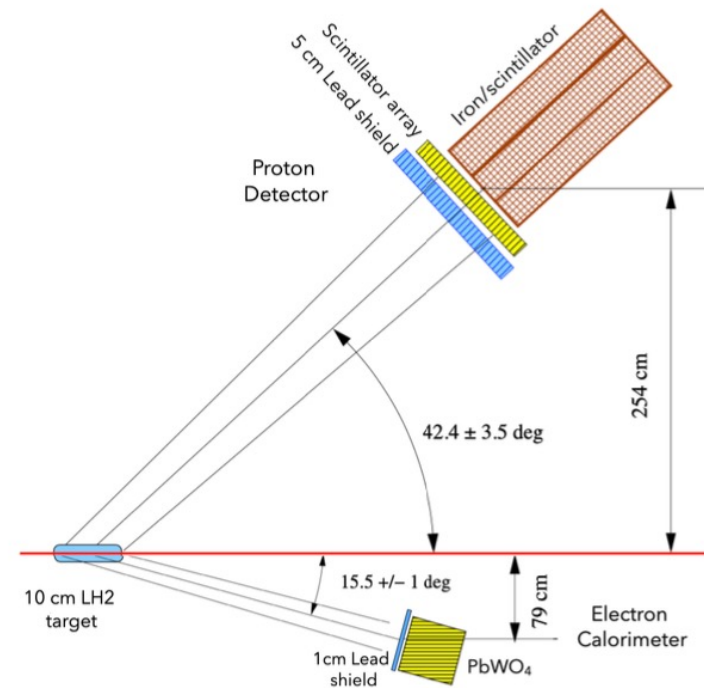
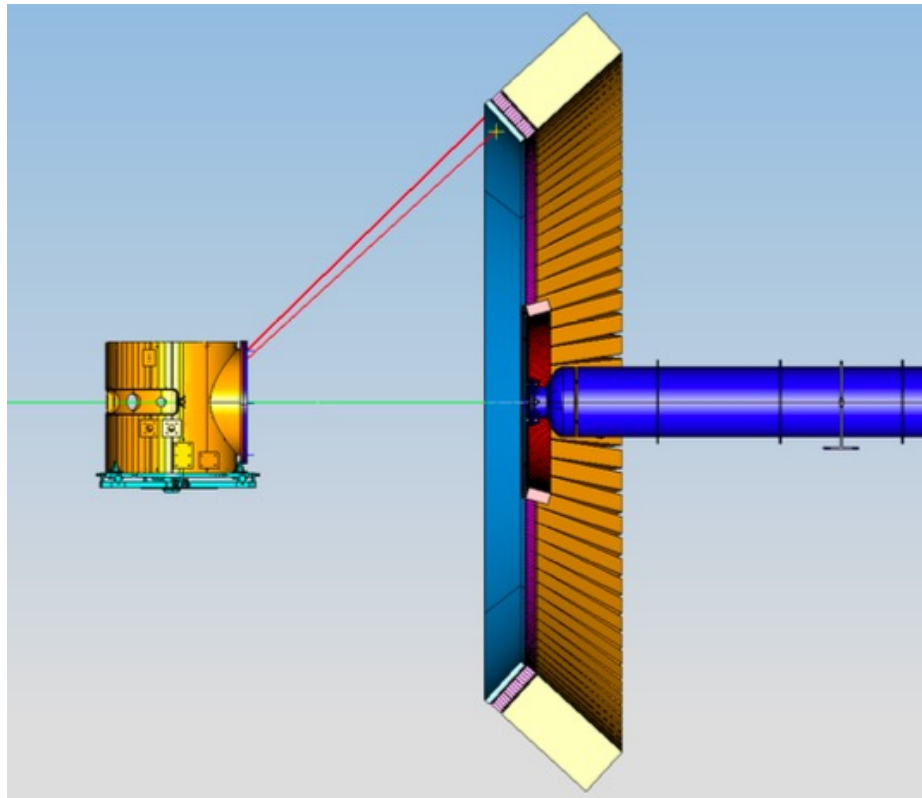
R. Beminiwattha, D. Hamilton, C. Palatchi, K. Paschke, B. Wojtsekhowski

$$A_{PV} = -\frac{G_F Q^2}{4\pi\alpha\sqrt{2}} \cdot \left[(1 - 4\sin^2\theta_W) - \frac{\epsilon G_E^p G_E^n + \tau G_M^p G_M^n}{\epsilon(G_E^p)^2 + \tau(G_M^p)^2} - \frac{\epsilon G_E^p G_E^s + \tau G_M^p G_M^s}{\epsilon(G_E^p)^2 + \tau(G_M^p)^2} \right. \\ \left. + \epsilon'(1 - 4\sin^2\theta_W) \frac{G_M^p G_A^{Zp}}{\epsilon(G_E^p)^2 + \tau(G_M^p)^2} \right]$$

Discovery potential – non zero sFF



Nonzero Strange FF, E12-23-004

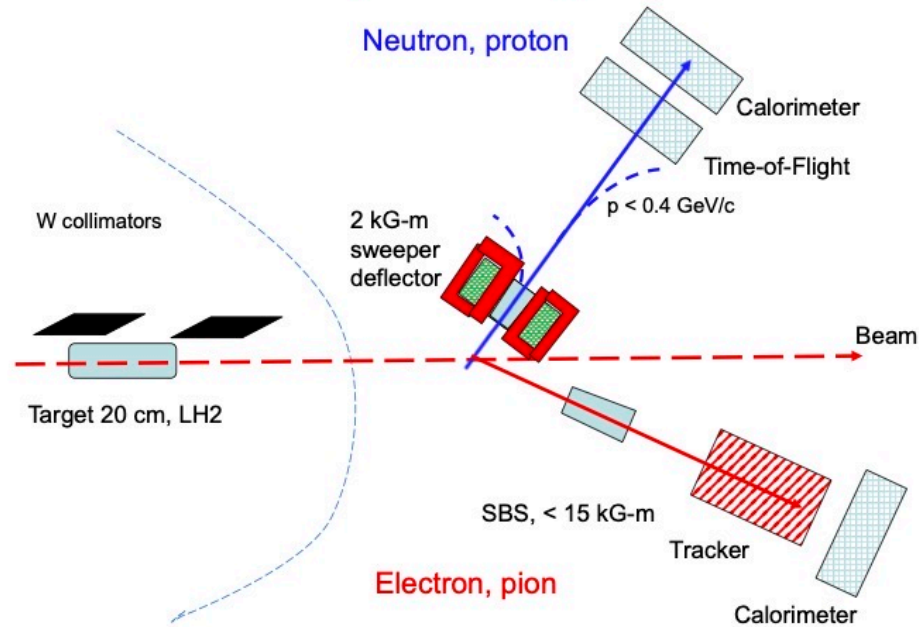


Axial-Vector Form Factor

T. Averett, J. Napolitano, B. Wojtsekhowski, W. Xiong

$$e + p \Rightarrow \nu + n$$

Layout of experiment



high energy
threshold!

100 ps TOF

Challenges in the study $e + p \rightarrow \nu + n$

- Cross section for the weak process is $\sim 10^{-39} \text{ cm}^2/\text{sr}$
- Pion photo-production cross section $\sim 10^8$ of the weak one
- Proton rate from electron elastic e-p $\sim 10^7$ of the weak one

The solutions are

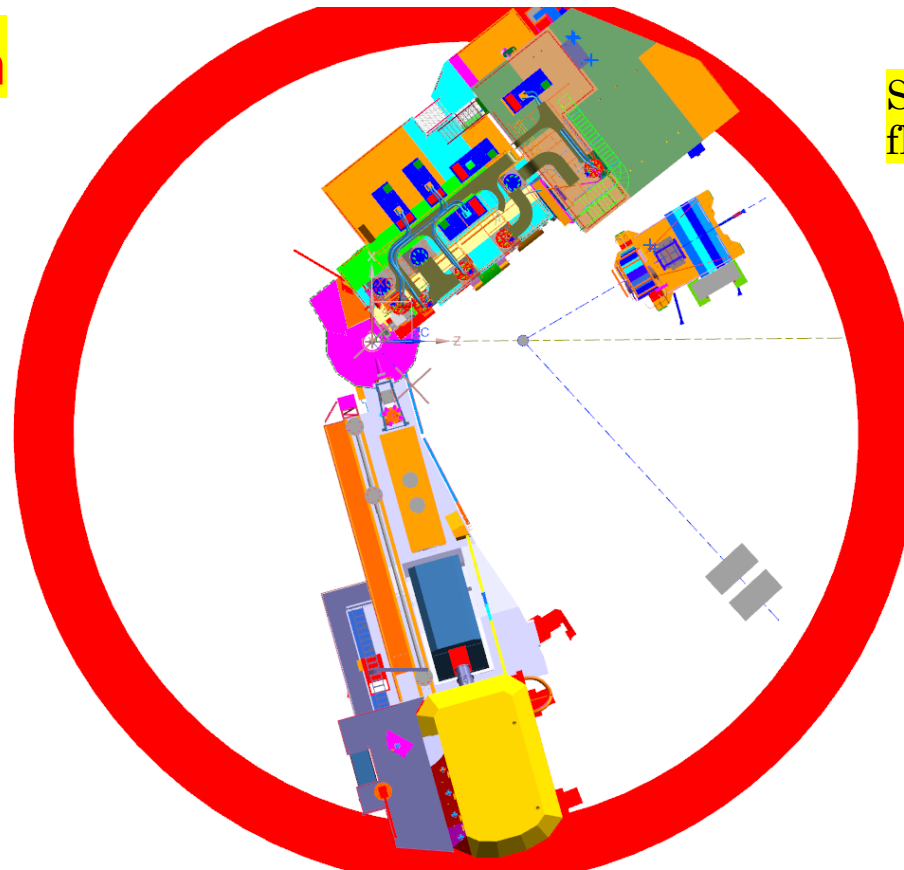
- 1) **High resolution TOF, 100 ps** => selection elastic recoiled neutrons
It allows us to reduce relevant photon energy range to 1% near the end-point and, as result, the pion-neutron rate, esp. due to 2% shift (pion mass effect).
- 2) **Veto of the high momentum pion** in SBS – a factor 10+ (limited by pion decay)
- 3) **Helicity asymmetry** is 100% for the signal and of 10^{-7} for the pion channel.

$$N_\nu = N_+ - N_- \quad N_\nu = 20k \pm 5k$$

Axial-Vector Form Factor

T. Averett, J. Napolitano, B. Wojtsekhowski, W. Xiong

$$e + p \Rightarrow \nu + n$$



Steve's design:
flipped the arms

high energy
threshold!

100 ps TOF

Polarized WACS, E12-17-008

D. Day, D. Hamilton, D. Keller, G. Niculescu, B. Wojtsekhowski, J. Zhang

- 1 A $2.5 \mu\text{A}$ polarized electron beam incident on a 10 % radiator inside a new Compact Photon Source (CPS) produces a high-intensity untagged photon beam.
- 2 The proton target is the UVA/JLab solid polarized ammonia target.
- 3 The recoil proton is detected with the BigBite spectrometer equipped with GEM trackers and trigger detectors.
- 4 The highly-segmented PbWO_4 NPS calorimeter is used to detect the scattered photon.

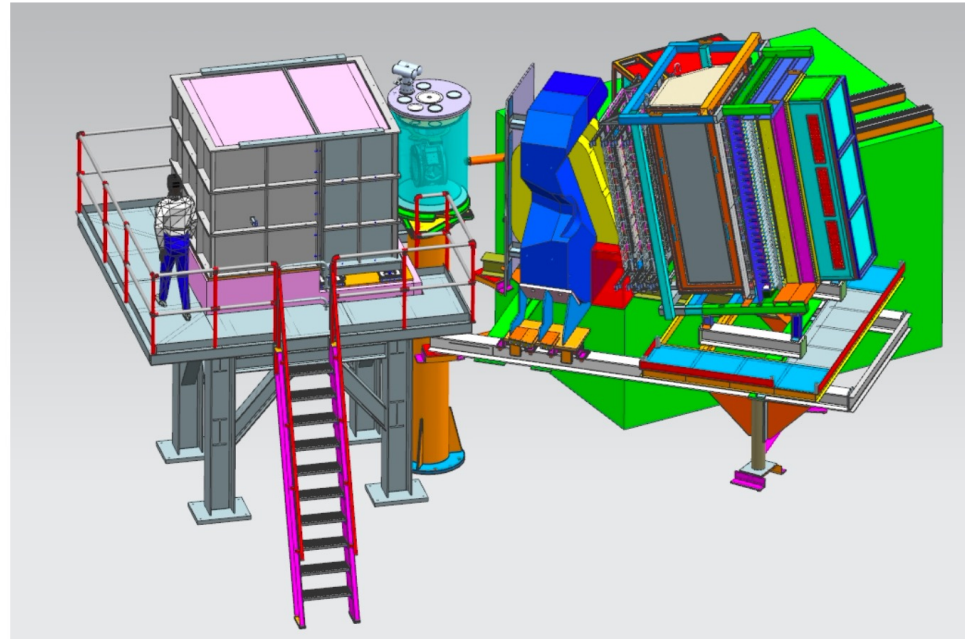


Figure from Steve Lassiter

The use of the CPS and BigBite results in a factor of 30 improvement in figure-of-merit over previous experiments and opens up a new range of polarized physics opportunities at JLab.

Polarized WACS, CPS

A conceptual design study of a Compact Photon Source (CPS) for Jefferson Lab Lab NIM-A 957 (2020) 163429

D. Day^a, P. Degtiarenko^b, S. Dobbs^c, R. Ent^b, D.J. Hamilton^d, T. Horn^{e,b,*}, D. Keller^a,
C. Keppel^b, G. Niculescu^f, P. Reid^g, I. Strakovsky^h, B. Wojtsekhowski^b, J. Zhang^a

D. Day, P. Degtiarenko, S. Dobbs et al.

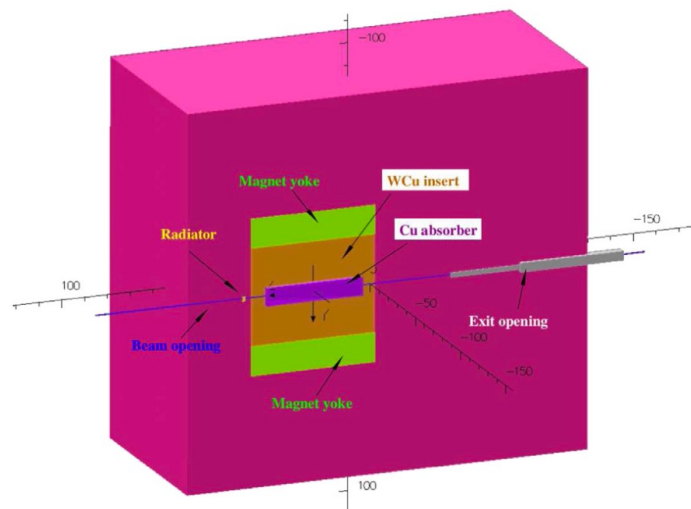


Fig. 3. The CPS cut-out side view. Deflected electrons strike a copper absorber, surrounded by a W-Cu insert inside the magnet yoke. The outer rectangular region in this view is the tungsten-powder shield.

Nuclear Inst. and Methods in Physics Research, A 957 (2020) 163429

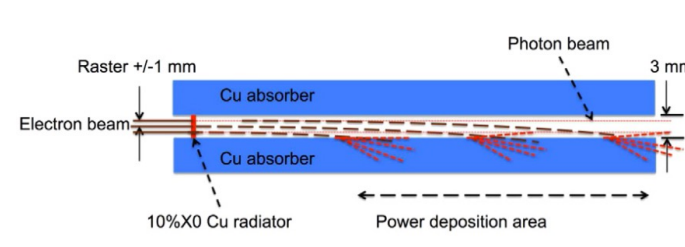


Fig. 4. The scheme of beam deflection in the magnetic field to the absorber/dump.

around the photon beam can be as narrow as the photon beam size. After passing through the radiator, the electron beam should be separated from the photon beam by means of deflection in a magnetic field. The length, aperture and field strength of the magnet are very different in the proposed source compared to in the traditional tagging technique. In the traditional source the magnet is needed to direct the electrons to the dump. Because of the large momentum spread of electrons which

Polarized WACS, E12-17-008

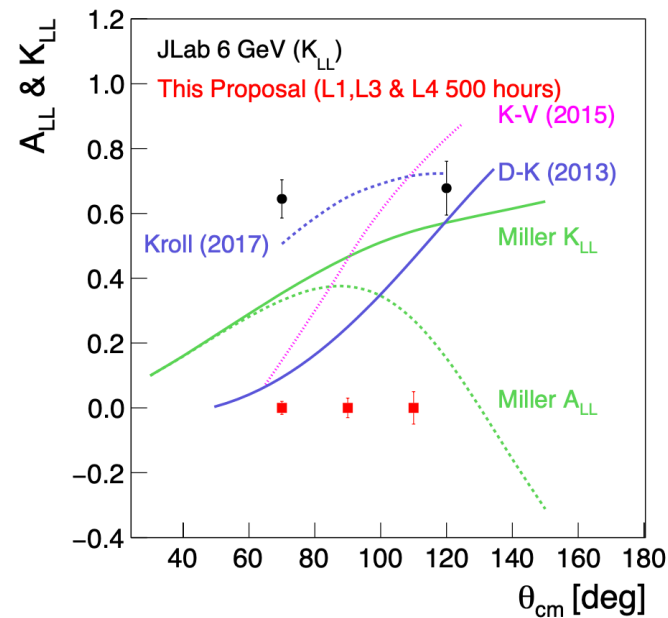
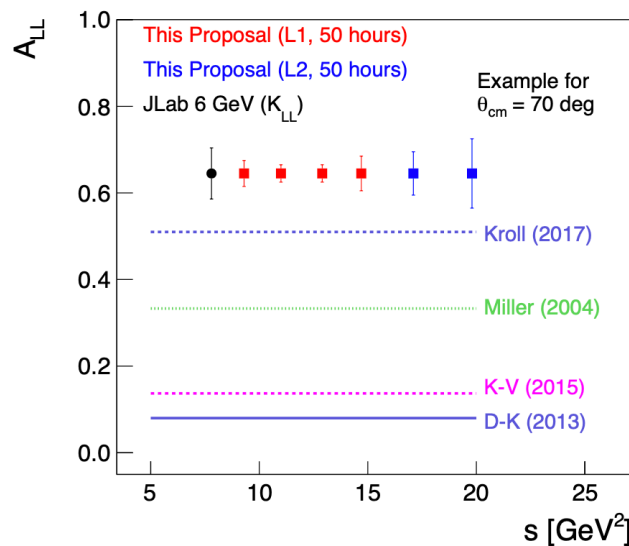
$$\frac{d\sigma}{dt} = \left(\frac{d\sigma}{dt} \right)_{\text{KN}} \left\{ \frac{1}{2} \frac{(s-u)^2}{s^2+u^2} \left[R_V^2(t) + \frac{-t}{4m^2} R_T^2(t) \right] + \frac{1}{2} \frac{t^2}{s^2+u^2} R_A^2(t) \right\}$$

$$A_{LL} = K_{LL} \Rightarrow \frac{R_A(t)}{R_V(t)} A_{LL}^{\text{KN}}$$

$$A_{LS} = -K_{LS} = A_{LL} \left[\frac{\sqrt{-t}}{2m} \frac{R_T(t)}{R_V(t)} - \beta \right]$$

Diehl & Kroll, EPJ C73 (2013)

Axial FF again



Experiments on the polarized targets

- Polarized Wide Angle Compton Scattering, E12-17-008
- Pion photoproduction from neutron – replacement of ALL/He-3
- Polarized deuteron to p-n – higher photon energy
- Pion photoproduction from proton
- T20 in polarized D(e,e'd) – 10-20x larger solid angle
- Proton g_1/g_2 – BB/SBS has large solid angle and tracking
- High-x A1/A2 using He-3 and SBS/BB

Tensor Polarized D(e, e' d)



ELSEVIER

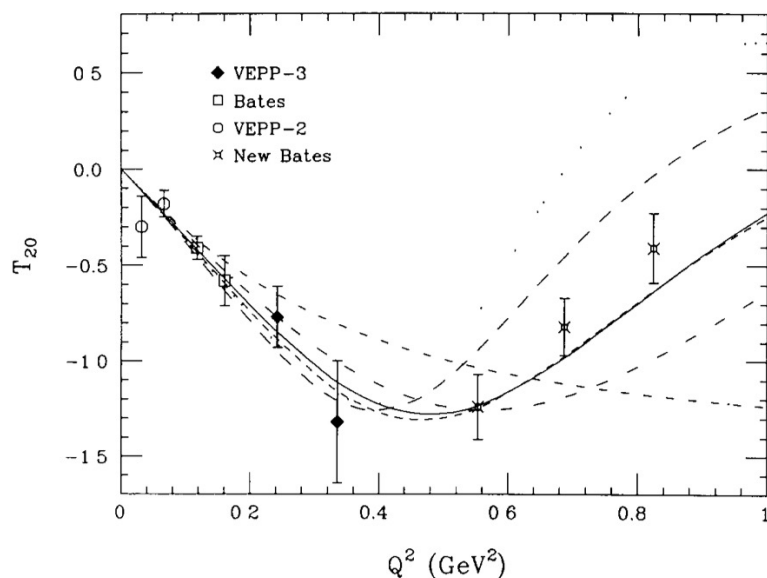
Nuclear Instruments and Methods in Physics Research A 350 (1994) 423-429

NUCLEAR
INSTRUMENTS
& METHODS
IN PHYSICS
RESEARCH
Section A

An active storage cell for a polarized gas internal target

K.P. Coulter^{a,*1}, R. Gilman^{a,2}, R.J. Holt^a, L.G. Isaeva^b, E.R. Kinney^{a,3}, R.S. Kowalczyk^a,
S.I. Mishnev^b, J. Napolitano^{a,4}, D.M. Nikolenko^b, S.G. Popov^b, D.H. Potterveld^a,
I.A. Rachek^b, A.V. Sukhanov^b, A.B. Temnykh^b, D.K. Toporkov^b, E.P. Tsentalovich^b,
B.B. Wojtsekhowski^b, L. Young^a, A. Zghiche^a

R. Gilman et al. / Polarized gas target using a storage cell



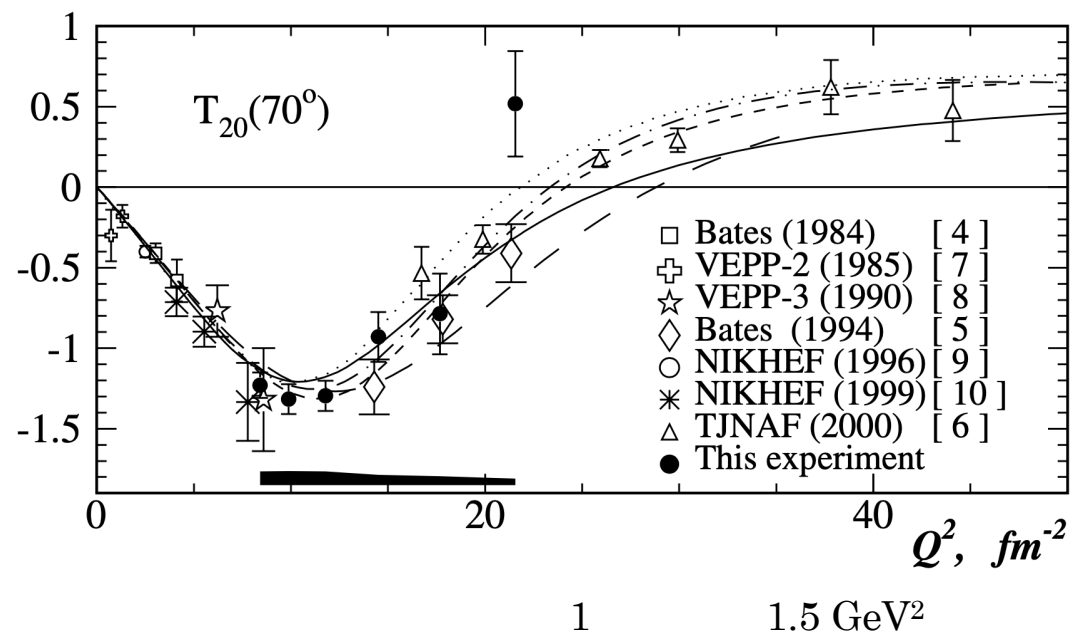
VOLUME 90, NUMBER 7

PHYSICAL REVIEW LETTERS

week ending
21 FEBRUARY 2003

Measurement of the Tensor Analyzing Powers T_{20} and T_{21} in Elastic Electron-Deuteron Scattering

D. M. Nikolenko,¹ H. Arenhövel,² L. M. Barkov,¹ S. L. Belostotsky,³ V. F. Dmitriev,¹ M. V. Dyug,¹ R. Gilman,^{4,5}
R. J. Holt,⁶ L. G. Isaeva,¹ C. W. de Jager,^{7,5} E. R. Kinney,⁸ R. S. Kowalczyk,⁶ B. A. Lazarenko,¹ A. Yu. Loginov,⁹
S. I. Mishnev,¹ V. V. Nelyubin,³ A. V. Osipov,⁹ D. H. Potterveld,⁶ I. A. Rachek,¹ R. Sh. Sadykov,¹ Yu. V. Shestakov,¹
A. A. Sidorov,⁹ V. N. Stibunov,⁹ D. K. Toporkov,¹ V. V. Vikhrov,³ H. de Vries,⁷ and S. A. Zevakov¹



Tensor Polarized D(e, e' d)



Nuclear Instruments and Methods in Physics Research A 350 (1994) 423-429

NUCLEAR
INSTRUMENTS
& METHODS
IN PHYSICS
RESEARCH
Section A

An active storage cell for a polarized gas internal target

K.P. Coulter^{a,*1}, R. Gilman^{a,2}, R.J. Holt^a, L.G. Isaeva^b, E.R. Kinney^{a,3}, R.S. Kowalczyk^a,
S.I. Mishnev^b, J. Napolitano^{a,4}, D.M. Nikolenko^b, S.G. Popov^b, D.H. Potterveld^a,
I.A. Rachek^b, A.V. Sukhanov^b, A.B. Temnykh^b, D.K. Toporkov^b, E.P. Tsentalovich^b,
B.B. Wojtsekhowski^b, L. Young^a, A. Zghiche^a

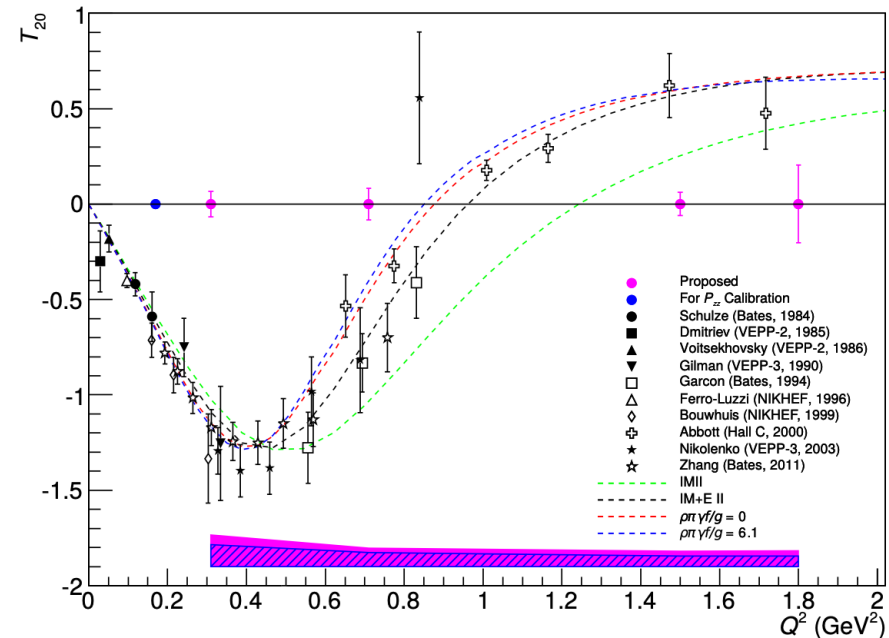
Luminosity internal target:

100 mA x 1×10^{13} atoms/cm²

$L \sim < 1 \times 10^{32}$ Hz/cm²

Solid ND₃ => $L \sim 1 \times 10^{34}$ Hz/cm²

Approved experiment
E12-15-005 (HMS/SHMS)



SBS/BB provide **10x larger** solid angle than HMS/SHMS

Double polarized $H(\gamma, \pi^0 + p)$

SBS allows
FM gain 20+

K. WIJESORIYA *et al.*

PHYSICAL REVIEW C 66, 034614 (2002)

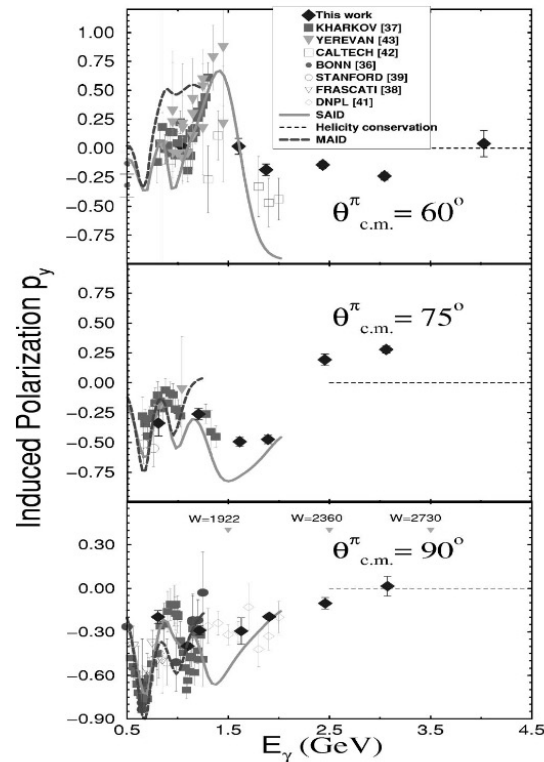


FIG. 9. Top to bottom: Induced polarization p_y in neutral pion photo-production at $\theta_{c.m.} = 60^\circ$, 75° , and 90° . Only statistical uncertainties are shown. The three curves, SAID [22], MAID [23], and helicity conservation shown in the figures are described in the text. Corresponding W range is also shown in the bottom plot.

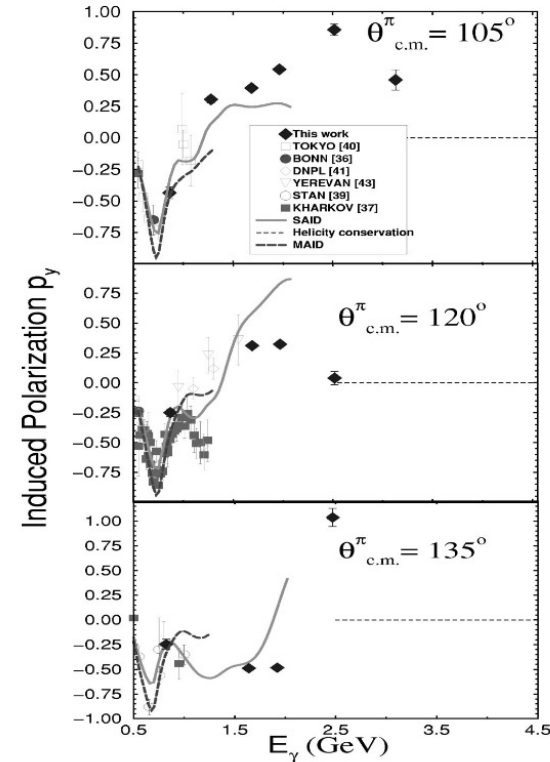


FIG. 10. Top to bottom: Induced polarization p_y in neutral pion photo-production at $\theta_{c.m.} = 105^\circ$, 120° , 135° . Only statistical uncertainties are shown. The three curves SAID [22], MAID [23], and helicity conservation shown here are described in the text.

Double polarized $D(\gamma, p + n)$

VOLUME 86, NUMBER 14

PHYSICAL REVIEW LETTERS

2 APR

SBS allows
FM gain 20+

Polarization Measurements in High-Energy Deuteron Photodisintegration

K. Wijesooriya,^{10,*} A. Afanasev,^{20,26} M. Amarian,¹¹ K. Aniol,³ S. Becher,⁹ K. Benslama,²³ L. Bimbot,²² P. Bosted,¹⁶

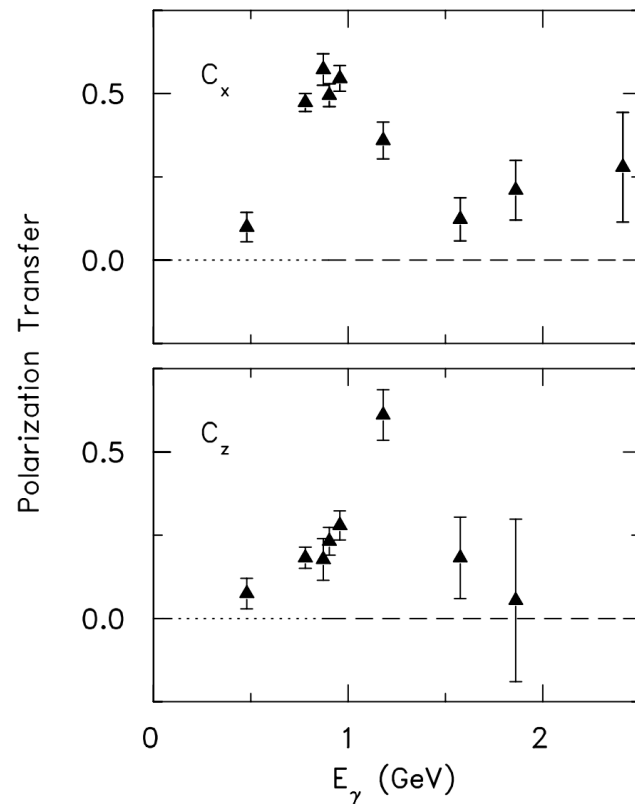


FIG. 2. Polarization transfers C_x and C_z in deuteron photodisintegration at $\theta_{c.m.} = 90^\circ$. Only statistical uncertainties are shown.

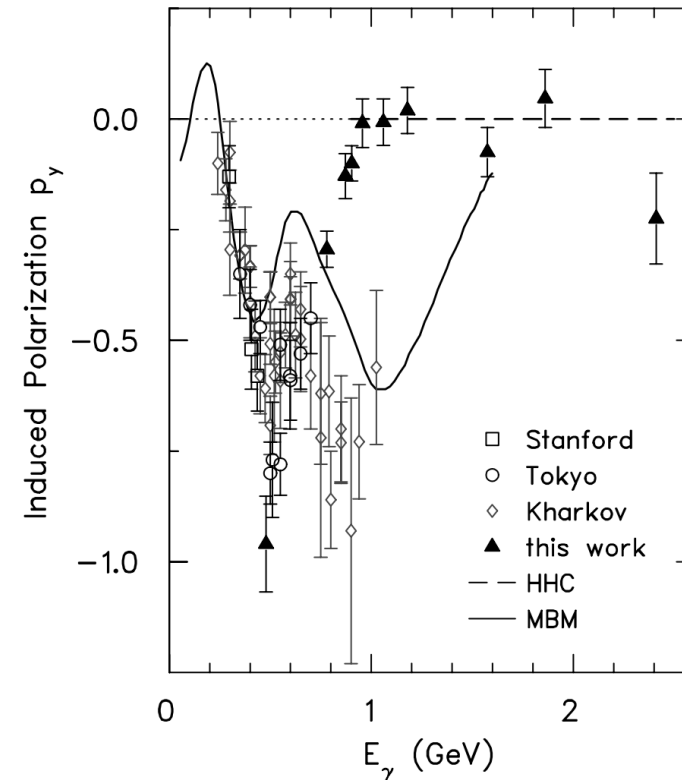


FIG. 1. Induced polarization p_y in deuteron photodisintegration at $\theta_{c.m.} = 90^\circ$. Only statistical uncertainties are shown. The curves are described in the text.

High energy $D(\gamma, p + n)$

SBS allows
FM gain 20+

VOLUME 87, NUMBER 10

PHYSICAL REVIEW LETTERS

3 SEPTEMBER

Measurement of the High Energy Two-Body Deuteron Photodisintegration Differential Cross Section

E. C. Schulte,¹ A. Ahmidouch,² C. S. Armstrong,³ J. Arrington,⁴ R. Asaturyan,⁵ S. Avery,⁶ O. K. Baker,^{3,6} D. H. Beck,¹ H. P. Blok,⁷ C. W. Bochna,¹ W. Boeglin,⁸ P. Y. Bosted,⁹ M. Bouwhuis,¹ H. Breuer,¹⁰ D. S. Brown,¹⁰

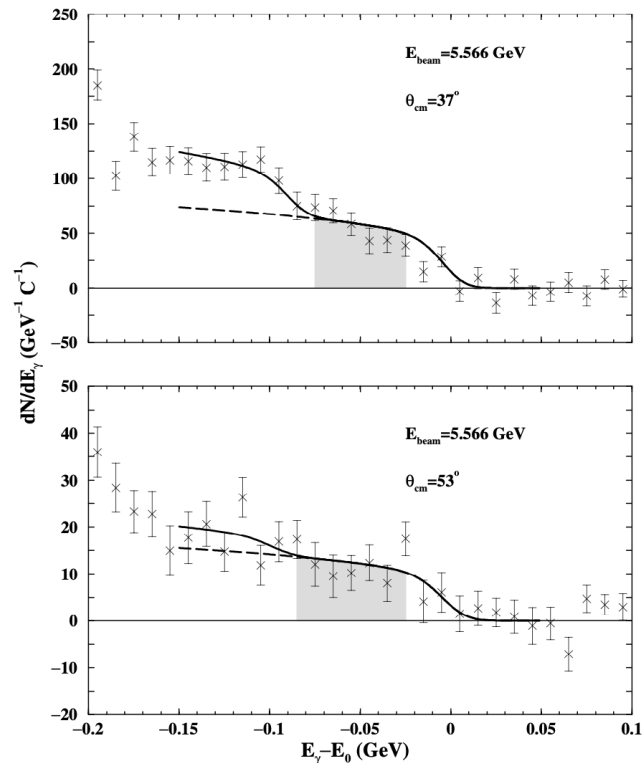


FIG. 1. Photon energy spectra, normalized to collected electron beam charge, for $\theta_{\text{cm}} = 37^\circ$ (top panel) and 53° (bottom panel) at 5.5 GeV. The grey shaded area denotes the region in E_γ where the photoproton yield is calculated. The curves are described in the text.

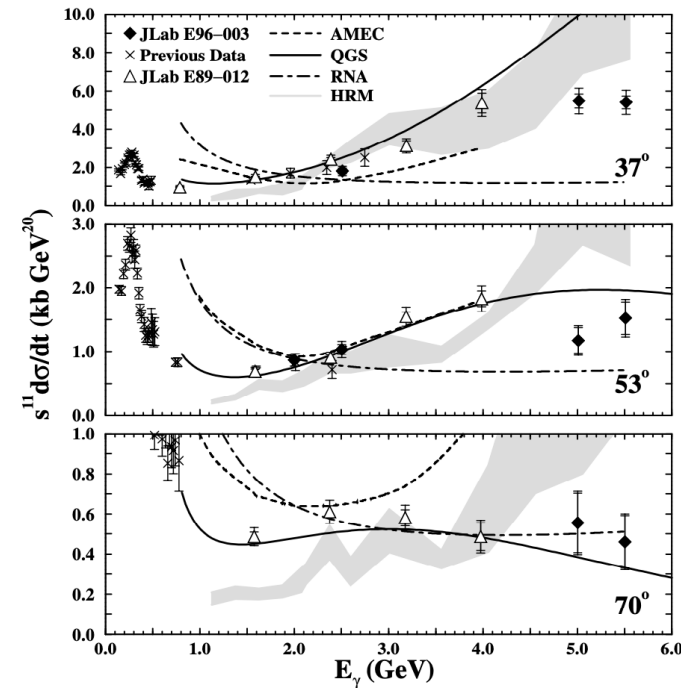


FIG. 2. $s^{11} \frac{d^2\sigma}{dt^2}$ vs E_γ for $d(\gamma, p)n$. The present data are shown as solid diamonds. Errors for JLab data are statistical and total errors. All others are statistical only. E89-012 data are shown as open triangles. All other data are shown as crosses and are as presented in Refs. [2,3,22]. The solid line is the QGS calculation [10]. The long-short dashed line is the RNA calculation [11]. The short dashed line is the AMEC [15]. The grey area is the HRM [9].

Summary

- ❖ SBS + BB provide a flexible instrument which is the best choice for many high-z high- Q^2 exclusive reactions.
- ❖ Compact Photon source boosts productivity with polarized NH_3/ND_3 by 10+ times.
- ❖ Approved experimental program is large and additional important physics proposals could be developed.